The π-conjugated P-flowers C16(PH)8 and C16(PF)8 are potential materials for organic n-type semiconductors

ARTICLE *in* PHYSICAL CHEMISTRY CHEMICAL PHYSICS · AUGUST 2012

Impact Factor: 4.49 · DOI: 10.1039/c2cp42474f · Source: PubMed

3 AUTHORS, INCLUDING:

Truong Tai
University of Leuven
67 PUBLICATIONS **524** CITATIONS
SEE PROFILE

Minh Tho Nguyen
University of Leuven
750 PUBLICATIONS **11,206** CITATIONS
SEE PROFILE

PCCP

Dynamic Article Links

Cite this: *Phys. Chem. Chem. Phys.*, 2012, **14**, 14832–14841

www.rsc.org/pccp

PAPER

The π-conjugated P-flowers $C_{16}(PH)_8$ and $C_{16}(PF)_8$ are potential materials for organic n-type semiconductors†

Vu Thi Thu Huong,[a] Truong Ba Tai[a] and Minh Tho Nguyen*[ab]

Received 30th May 2012, Accepted 1st August 2012
DOI: 10.1039/c2cp42474f

Following the theme of this special issue, two new compounds, the P-flowers $C_{16}(PH)_8$ and $C_{16}(PF)_8$, are designed by us and subsequently characterized by quantum chemical computations. Their geometries and infrared signatures are analyzed and compared to those of the well-known sulflower $C_{16}S_8$. Their electronic structure and aromaticity are examined using the electron localization function (ELF) and also by the total and partial densities of state (DOS). Both $C_{16}(PF)_6$ and $C_{16}(PH)_8$ molecules exhibit small energy barrier of electron injection (Φ_e = 0.33 eV for the gold electrode for the former, and Φ_e = 0.1 eV for the calcium electrode for the latter), remarkably low reorganization energy and high rate of electron hopping. Thus, both theoretically designed P-flower molecules are predicted to be excellent candidates for organic n-type semiconductors.

1. Introduction

Organic π-conjugated materials continue to attract much attention in both experimental and theoretical studies alike, in part due to their wide industrial applications, currently in the electronic devices such as organic field effect transistors (OFETs), organic thin film transistors (OTFTs), organic light emitting diodes (OLEDs), photovoltaic cells, sensors, *etc.*[1–3] During the past decades, numerous organic semiconductor materials have extensively been investigated.[4–8] Recent experimental studies showed that some organic p-type semiconductors such as pentacene, rubrene,[9,10]… have achieved a mobility beyond 10 $cm^2\ V^{-1}\ s^{-1}$, which is comparable to the mobility of amorphous silicon devices. However, such efficient organic materials have not been found yet for n-type semiconductors that are necessary to produce a complementary circuit being composed of both p-type and n-type semiconductors. A reason for this lack of a suitable product is the high barrier of electron injection and the intrinsic instability of the resulting radical anions in air. As a consequence, the search for an effective material to be used as an n-type semiconductor remains a real challenge. In this context, we have been searching for new molecules derived from the heterocycles phosphole and sulflower that can be considered for use as n-type semiconductors using quantum chemical computations.

Since experimentally prepared by Chernichenko *et al.*,[11] the octathio[8]-circulene $C_{16}S_8$, **1**, named *sulflower*, and its derivatives have extensively been investigated. Possessing highly conjugated π-electron systems and a large hole mobility, the sulflower **1** has been considered as a good candidate for use in the fabrication of organic electronic devices.[12–16] In fact, a theoretical investigation on $C_{16}S_8$ and its derivatives including $C_{16}S_4Se_4$, $C_{16}X_8$ with X = O, Se, NH and CH_2[17] showed that the three molecules $C_{16}S_8$, $C_{16}S_4Se_4$ and $C_{16}Se_8$ have low reorganization energies that are compatible to those of well-known hole-transport materials such as pentacene, tetracene and dithiophene-tetrathiafulvalene (DT-TTF). The remaining molecules $C_{16}X_8$ with X = CH_2, NH and O considered in this study[17] have rather convex forms and much higher reorganization energies.

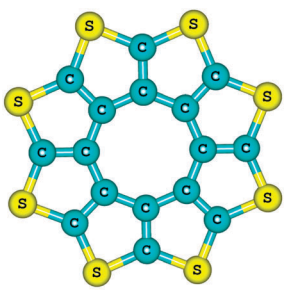

1 ($C_{16}S_8$, Sulflower)

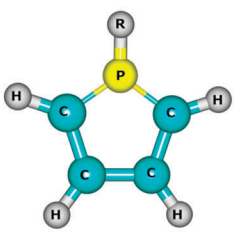

2 (Phospholes)

In previous studies, we demonstrated that replacement of the S atoms in thiophene moieties, giving rise to phosphole derivatives **2**, also leads to π-conjugated polymers with similar or even better optoelectronic properties.[18–22] We also showed that fluorination of the parent phosphole **2** (R = F) turns out to induce remarkable changes in the geometrical, thermochemical

[a] *Department of Chemistry, University of Leuven, Celestijnenlaan 200 F, B-3001 Leuven, Belgium. E-mail: minh.nguyen@chem.kuleuven.be*
[b] *Institute for Computational Science and Technology at HoChiMinh City (ICST), Quang Trung Software Park, HoChiMinh City, Vietnam*

† Electronic supplementary information (ESI) available: Tables containing the Cartesian coordinates of the optimized geometries. See DOI: 10.1039/c2cp42474f

and electronic properties, in such a way that the n-type and p-type oligomers could be obtained upon different arrangements of the building blocks.[23,24] The strong and polarized P–F bonds and the high electronegativity of the fluorine element are mostly responsible for the different changes.[24] Introduction of electron withdrawing groups such as F or CN, *etc.* into a p-type semiconductor molecule tends to decrease the energy levels of the highest occupied (HOMO) and the lowest unoccupied (LUMO) molecular orbitals, and also to increase the electron affinity of the resulting molecules.[4] Consequently, an n-type material can be obtained as the case of perfluoropentacene or fluorophospholes. Thus, an intriguing question is as to whether the P-derivatives of the sulflower **1**, namely the poly-phosphole $C_{16}(PH)_8$ **3** (all S atoms in **1** being replaced by PH groups) and its fluorinated derivative $C_{16}(PF)_8$ **4** (all S atoms in **1** being replaced by PF groups) also exhibit electronic properties similar to $C_{16}S_8$ **1**. At the first glance, the P–C bond length is longer than that of the N–C bond, but close to that of the S–C bond. Thus, it is expected that $C_{16}(PR)_8$ exhibit planar geometries and their electronic properties are closer to those of $C_{16}S_8$ than to those of the pyrazole derivatives $C_{16}(NR)_8$.

Motivated by the above reasons, we set out to perform theoretical investigations on $C_{16}(PX)_8$ **3** and **4** using quantum chemical calculations. Our theoretical results predict that both novel *P-flowers* $C_{16}(PH)_8$ **3** and $C_{16}(PF)_8$ **4** have quasi-planar structures and low reorganization energy. In what follows, we emphasize that these new low-coordinated P-molecules, if they could experimentally be prepared under good conditions, could be used to fabricate organic electronic devices with promising features.

2. Computational methods

All electronic structure calculations are carried out using the Gaussian 03[25] suite of programs. Optimizations of the relevant geometries and calculations of their harmonic vibrational frequencies are fully performed using density functional theory (DFT). Four different functionals, including B3LYP,[26–28] B3P86,[28,29] BLYP[26,27] and BHandHLYP functionals,[26,30] are used in conjunction with the 6-31G(d,p) basis sets.[31,32] The B3LYP and B3P86 are hybrid exchange–correlation functionals using Becke's three-parameter exchange B3 functional in which the fraction of Hartree–Fock (HF) exchange is 20%.[28] While BLYP is a pure GGA-functional using Becke's 1988 exchange functional,[26] the fraction of HF-exchange of the BHandHLYP is increased up to 50%.[30] The functional BP86 was successfully applied to predict the geometries and electronic properties of π-conjugated systems in recent studies.[8,13] Although the B3LYP functional was also commonly used,[7,8,12–14] the transfer integral obtained using this functional was overestimated in few cases.[13,33,34] The use of functionals with different fractions of Hartree–Fock exchange (0% for BLYP, 20% for B3LYP and B3P86 and 50% for BHandHLYP) allows the effect of HF exchange fraction on the computed properties of molecules to be evaluated. For each species considered, the neutral, anionic and cationic states are characterized. In order to compare the properties of our designed molecules **3** and **4** to those of **1** and other previously reported materials, single-point electronic energies of molecules are also carried out using the B3LYP/6-31++G(d,p) level of theory.[35]

The configurations of the dimers of compounds considered are investigated by using the B3LYP-D functional[36,37] in conjugation with the 6-31G(d) basis set. Inclusion of the dispersion energy (-D) is usually needed to describe the solid-state packing of molecules.[38] These calculations are performed using the Turbomole 6.3 software.[39]

In order to probe the molecular electronic structure, the total (DOS) and partial (pDOS) density of states are constructed using the MOs obtained at the B3LYP/6-311G(d) level. The delocalization and aromaticity of the π-electron systems are also examined using the topological analysis of the electron localization function (ELF). The ELF maps are generated using the B3LYP/6-311+G(d) densities and with the aid of the Dgrid-4.2 software.[40] The ELF plots are subsequently made using the Gopenmol software.[41]

3. Results and discussion

Stability and geometrical features of the isomers

The isomers of $C_{16}(PH)_8$ **3** and $C_{16}(PF)_8$ **4** are constructed by simply substituting each of sulfur atoms of **1** by either one PH- or PF-group. The only difference between these P-isomers is the position of R (H/F) atoms. While all R-atoms of the isomers **3A** and **4A** are pointed toward the same direction from the molecular plane, the R-atoms of **3B** and **4B** follow an up-down motif with a *trans*-configuration for two successive R atoms. Optimization of geometries and determination of harmonic vibrational frequencies of the structures are performed using DFT calculations. The same procedure is carried out for the cationic and anionic states. While the shapes of the isomers are depicted in Fig. 1, their geometrical parameters, point groups and relative energies are summarized in Table 1. Although both isomers of $C_{16}(PH)_8$ are located as local minima without imaginary frequencies, the isomer **3A** is more stable than **3B** in all the charged states considered. Of the neutrals, **3A** is 2.7 kcal mol^{-1} more stable than **3B** (B3LYP/6-31G(d,p)). This gap is increased to

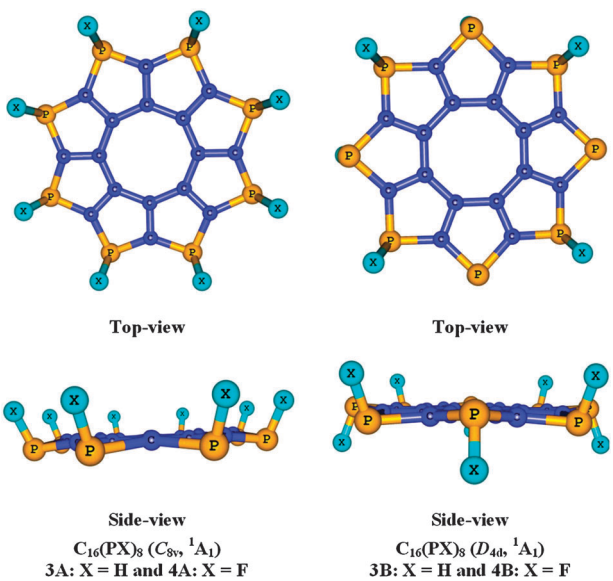

Fig. 1 Shapes of isomers $C_{16}(PH)_8$ and $C_{16}(PF)_8$.

Table 1 Relative energies (kcal mol^{-1}), selected geometrical parameters (Å) and symmetry point groups of isomers $C_{16}(PH)_8$ and $C_{16}(PF)_8$ in neutral, anionic and cationic states

Molecule		**3A**	**3B**	**4A**	**4B**
Neutrals					
Point group and electronic state		**3A** C_{8v} $^1A_1$	**3B** D_{4d} $^1A_1$	**4A** C_{8v} $^1A_1$	**4B** D_{4d} $^1A_1$
Relative energy	BLYP/6-31G(d,p)	0.00	3.1	0.0	12.6
	B3LYP/6-31G(d,p)	0.0	2.7	0.0	11.3
	B3P86/6-31G(d,p)	0.0	2.9	0.0	13.5
	BHandHLYP/6-31G(d,p)	0.0	2.1	0.0	8.8
C–P distance (d_{P-C})	BLYP/6-31G(d,p)	1.822	1.825	1.820	1.826
	B3LYP/6-31G(d,p)	1.808	1.811	1.807	1.813
	B3P86/6-31G(d,p)	1.798	1.801	1.796	1.802
	BHandHLYP/6-31G(d,p)	1.797	1.799	1.798	1.805
Cations					
Point group and electronic state		**3A**$^+$ C_{2v} $^2B_1$	**3B**$^+$ C_2 ^2A	**4A**$^+$ C_{2v} $^2B_1$	**4B**$^+$ D_{4d} $^2A_2$
Relative energy	BLYP/6-31G(d,p)	0.0	3.3	0.0	3.7
	B3LYP/6-31G(d,p)	0.0	2.8	0.0	1.3
	B3P86/6-31G(d,p)	0.0	3.0	0.0	3.9
	BHandHLYP/6-31G(d,p)	0.0	2.4	0.0	0.9
C–P distance (d_{P-C})	BLYP/6-31G(d,p)	1.809–1.829	1.832	1.829–1.830	1.836
	B3LYP/6-31G(d,p)	1.794–1.814	1.795–1.817	1.793–1.815	1.823
	B3P86/6-31G(d,p)	1.783–1.804	1.785–1.807	1.780–1.803	1.811
	BHandHLYP/6-31G(d,p)	1.782–1.804	1.783–1.806	1.733–1.808	1.815
Anions					
Point group and electronic state		**3A**$^-$ C_{8v} $^2A_1$	**3B**$^-$ D_{4d} $^2A_2$	**4A**$^-$ C_{8v} $^2A_1$	**4B**$^-$ D_{4d} $^2B_2$
Relative energy	BLYP/6-31G(d,p)	0.0	3.8	0.0	10.9
	B3LYP/6-31G(d,p)	0.0	3.6	0.0	10.1
	B3P86/6-31G(d,p)	0.0	3.8	0.0	11.9
	BHandHLYP/6-31G(d,p)	0.0	3.7	0.0	9.8
C–P distance (d_{P-C})	BLYP/6-31G(d,p)	1.823	1.825	1.819	1.826
	B3LYP/6-31G(d,p)	1.808	1.810	1.806	1.812
	B3P86/6-31G(d,p)	1.799	1.801	1.795	1.802
	BHandHLYP/6-31G(d,p)	1.796	1.800	1.795	1.800

2.8 kcal mol^{-1} for cations and 3.6 kcal mol^{-1} for anionic species. The same predictions are made when the B3P86, BLYP and BHandHLYP functionals are used (Table 1).

Similar observations are also found for $C_{16}(PF)_8$ **4** that the isomer **4A** is 11.3 kcal mol^{-1} more stable than the isomer **4B**. In the anionic state, the radical **4A**$^-$ is also 10.1 kcal mol^{-1} lower in energy than the **4B**$^-$. This value is reduced to 1.3 kcal mol^{-1} for the energy difference between both cations **4A**$^+$ and **4B**$^+$.

In good agreement with previous reports, our calculations show that the two functionals B3LYP and B3P86 give similar geometrical parameters (Table 1). Interestingly, decrease of the HF-exchange leads to an increase in geometrical parameters. At the B3LYP/6-31G(d,p) level, the C–P bond lengths of molecules **3A** and **4A** are equal to 1.808 and 1.807 Å, respectively. These distances are increased to 1.822 Å for **3A** and 1.820 Å for **4A** when the BLYP functional is used. Oppositely, increase of HF-exchange from 20% in B3LYP to 50% in BHandHLYP tends to shorten the C–P bonding lengths. The C–P distances of **3A** and **4A** obtained from the BHandHLYP functional are approximately 0.01 Å shorter than the B3LYP counterparts. Additionally, our predictions also point out that a replacement of the correlation functional of LYP by the P86 tends to shorten the C–P distances. The B3P86/6-31G(d,p) values of the C–P bond lengths of molecules **3** and **4** amount to 1.798 and 1.796 Å, respectively, that are shorter than the relevant B3LYP values, and are close to those obtained by BHandHLYP. Similar observations are found for other compounds **3B** and **4B** and their charged counterparts (Table 1). In order to evaluate the accuracy of the functionals used, the same calculations are carried out for the known compound **1** $C_{16}S_8$. C–S distances of **1** are also decreased with respect to increasing HF-exchange in functionals (BLYP = 1.783 Å, B3LYP = 1.766 Å, B3P86 = 1.755 Å, and BHandHLYP = 1.750 Å). Compared to the average experimental values based on X-ray structure (d_{C-S} = 1.761 Å–1.765 Å), the B3LYP shows thus a better agreement. While the BLYP value is overestimated, the BHandHLYP value is underestimated.

More importantly, the C–P bond lengths are comparable to the C–S bond length of 1.755 Å of **1** $C_{16}S_8$ and of course much longer than the value of 1.415 Å in $C_{16}(NH)_8$ (B3P86/6-31G(d,p)).[17] These differences are no doubt the main reason for the quasi-planarity of $C_{16}(PH)_8$ and $C_{16}(PF)_8$, whereas a convex form was found for $C_{16}(NH)_8$. Geometrical features of **4** $C_{16}(PF)_8$ remain almost unchanged as compared to those of **3** $C_{16}(PH)_8$. Their symmetry point groups are the same, while the difference of P–C bond lengths between **3** and **4** amounts only to 0.002 Å. More importantly perhaps, the geometrical parameters given in Table 1 reveal that the carbon and phosphorus atoms of **3** and **4** are only slightly distorted out of the molecular plane. Consequently, a close packing can be expected as in the case of the sulflower **1**.

Following either attachment or detachment of one electron, the geometries of anionic and cationic species are slightly distorted. Because the isomers **3A** and **4A** show a higher stability as compared to their corresponding isomers **3B** and **4B**, we only show in the following section the calculated results obtained for the former.

Vibrational frequencies and infrared spectra

Since the P-flowers $C_{16}(PH)_8$ and $C_{16}(PF)_8$ are unknown molecules, a theoretical infrared (IR) signature could be useful

for their future experimental identification. For this purpose, their vibrational frequencies and IR spectra are predicted using the hybrid B3LYP functional in conjunction with the 6-31G(d,p) basis set. A uniform scaling factor of 0.9627 is used in the calculated harmonic frequencies.[42] We would note that this method has widely been proven to be effective enough for predicting the vibrational spectra of organic compounds. Recently, it was also applied to assign the IR spectra of sulflower $C_{16}S_8$ and its derivatives.[13,43]

The IR spectra of **3A** $C_{16}(PH)_8$ and **4A** $C_{16}(PF)_8$ in the frequency range of 500 to 1200 cm^{-1} are shown in Fig. 2a and b, respectively. The highest intensity peak centered at 1064 cm^{-1} and the lower peak at 884 cm^{-1} of the IR spectrum of **3A** correspond to the in-plane vibration modes of carbon and phosphorus atoms. The four remaining peaks with low intensities at 584, 711, 777 and 788 cm^{-1} are characteristic of out-plane vibration modes of C and P atoms. The two peaks with very high intensities observed at 2280 and 2282 cm^{-1} correspond to asymmetric and symmetric stretching vibrations of P–H groups. These values are comparable to the experimental values in the gas phase at 2328 cm^{-1} for asymmetric and 2323 cm^{-1} for symmetric vibration of PH_3.[44]

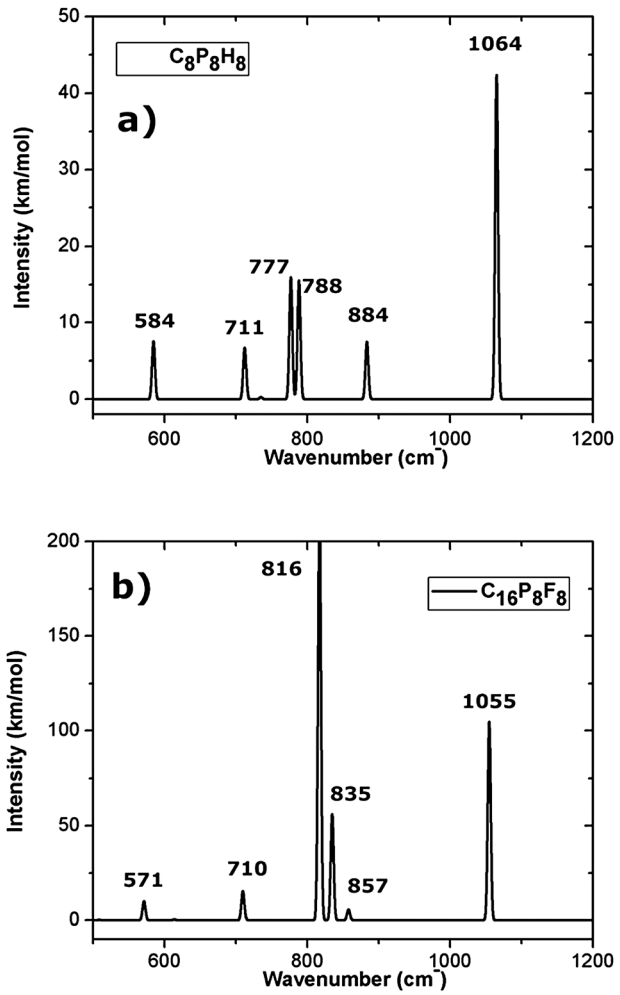

Fig. 2 Infrared spectra given in wave number (cm^{-1}) of (a) **3A** $C_{16}(PH)_8$ and (b) **4A** $C_{16}(PF)_8$ obtained at the B3LYP/6-311G(d) level.

The $C_{16}(PF)_8$ **4A** presents three high intensity peaks located at 1055, 835 and 816 cm^{-1} and three other peaks with lower intensities at 857, 710 and 571 cm^{-1}. The two peaks at 816 and 835 cm^{-1} correspond to the typical P–F asymmetric and symmetric vibrations. The latter are also comparable to the experimental values in the gas phase at 860 and 892 cm^{-1} for asymmetric and symmetric vibrations of gas phase PF_3.[44] Similar to $C_{16}(PH)_8$, the two peaks located at 1055 and 857 cm^{-1} in **4A** represent the in-plane C–P vibration modes, while the two remaining peaks at 571 and 710 cm^{-1} correspond rather to out-plane vibrational modes.

Electron delocalization and aromaticity

Features of electron delocalization and aromaticity of the π-electron system are relevant for the search of organic semiconductors. In this context, we examine these features of the molecules considered using the electron localization function (ELF) indices. This was applied effectively to evaluate the electron delocalization of organic compounds and also molecular clusters in the recent literature. The ELF that was proposed by Becke and Edgecombe[45] and supplemented by a determination of the ELF topological bifurcation[46] is a local measure of the Pauli repulsion between electrons due to the exclusion principle in 3D space. The definition of ELF is given by the following equations.

$$\mathrm{ELF} = \frac{1}{1 + \left(\frac{D_\mathrm{p}}{D_\mathrm{h}}\right)^2} \quad (1)$$

$$D_\mathrm{p} = \frac{1}{2}\sum_{i=1}^{N} |\nabla \Psi_i|^2 - \frac{1}{8}\frac{|\nabla \rho|^2}{\rho}$$

$$D_\mathrm{h} = \frac{3}{10}(3\pi^2)^{2/3}\rho^{5/3}$$

$$\rho = \sum_{i=1}^{N} |\psi_i(r)|^2$$

where D_p and D_h are the local kinetic energy density due to the Pauli exclusion principle, and the Thomas–Fermi kinetic energy density, respectively, and ρ is the electron density. These quantities can be evaluated using either Hartree–Fock or Kohn–Sham orbitals.

The total ELF maps can then be partitioned in terms of separate ELF_σ and ELF_π components that arise from the contributions of σ and π electrons, respectively. The latter can be used as useful indices describing the aromaticity of cyclic molecules.[47] Accordingly, a π aromatic ring possesses a high bifurcation value of ELF_π, whereas the corresponding bifurcation value in an anti-aromatic system is very low.

The ELF_π isosurfaces of molecules **3A** $C_{16}(PH)_8$, **4A** $C_{16}(PF)_8$ and **1** $C_{16}S_8$ are depicted in Fig. 3 together with their bifurcation values. At the first glance, it can be observed that all molecules exhibit good electron delocalization with contractors uniformly distributed over the entire systems. While the large basins located on either phosphorus or sulfur atoms correspond to their lone pairs, the smaller basins are distributed over the molecular frameworks and thus responsible

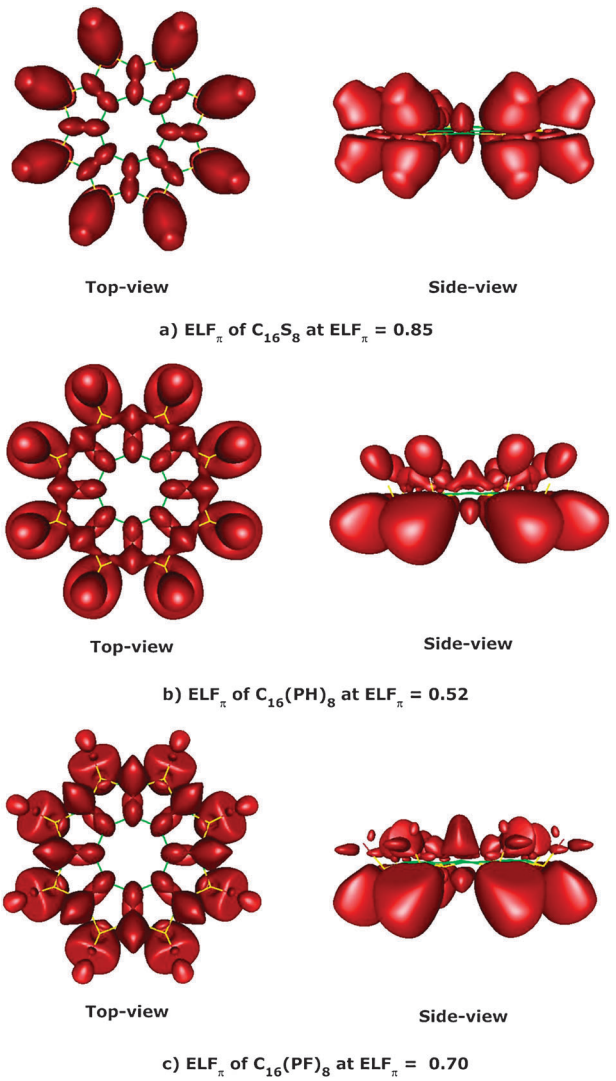

Fig. 3 The isosurfaces of ELF_π of (a) **1** $C_{16}S_8$, (b) **3A** $C_{16}(PH)_8$ and (c) **4A** $C_{16}(PF)_8$ at various bifurcation values.

for the molecular aromaticity. More importantly, our analysis reveals that **1** has a high bifurcation value of 0.85 that approximates to the value of 0.91 of benzene.[48] **4A** also exhibits a high ELF_π value of 0.70 that is comparable to the value of 0.75 of coronene.[48] Although **3A** $C_{16}(PH)_8$ presents a lower ELF_π value of 0.52, this value is still higher than that of 0.35 of typically anti-aromatic compound C_8H_8 (and 0.11 of C_4H_4).[48] As a consequence, both P-flower molecules **3** and **4** can be considered as moderately aromatic systems with good electron delocalization.

Frontier molecular orbital, ionization potential and electron affinity

Frontier molecular orbitals (HOMO and LUMO) play an important role in probing organic semiconductors. In experimental studies, gold (Au) with a work function of ~5.1 eV under vacuum is usually taken as the electrode of OFETs. Experimental results on OFETs showed that these devices have high performance when using Au as the electrodes.[4] In this case, the barriers of charge injection into Au electrodes can be defined as:

$$\text{electron injection } \Phi_e = 5.1 - |\text{LUMO}|,$$

and

$$\text{hole injection } \Phi_h = |\text{HOMO}| - 5.1.$$

For n-type organic semiconductors, an effective injection of electrons into the LUMO of the molecule is expected to happen when the molecule has a small Φ_e and a high enough electron affinity (EA). Proceeding in the opposite side, a low ionization energy (IE) and a small Φ_h value are required to allow an effective injection of holes from the HOMO of the molecule into the electrodes. However, because the n-type organic semiconductors with a high LUMO energy level are rather rare, some other metals such as calcium with a work function of 2.9 eV and magnesium with a work function of 3.68 eV are often used as electrodes.[4]

While the frontier molecular orbital (FMO) energy levels of the molecules considered are given in Table 2, their shapes are depicted in Fig. 4. The FMO energy levels of known compounds such as $C_{16}S_8$, pentacene (**PEN**) and perfluoropentacene (**PF-PEN**) are also computed using the same method. As the latter compounds were investigated in experimental studies,[15,49–51] their results allow us to calibrate the computational methods, and also to probe applicability of the proposed molecules **3A** and **4A**. In addition, FMO energy levels of all compounds considered are also calculated by using the long-range-separated functional LC-BLYP[52] that was reported to be very effective to compute the FMO energy level of π-conjugated molecules.[53] Compared to the experimental HOMO energy levels of **1** $C_{16}S_8$, **PEN** and **PF-PEN** that were measured in solution, BLYP values are overestimated, while LC-BLYP values are underestimated. An opposite trend is found for their LUMO energy levels. As a consequence, the HOMO–LUMO gaps obtained from BLYP calculations become too small and those obtained from LC-BLYP too large. In this context, it is really not clear over the best choice for evaluating FMO energy levels.

For HOMO energies, the B3P86 reveals a good agreement for **PEN** and **PF-PEN**. The computed HOMO energies of

Table 2 The energy levels (eV) of HOMO and LUMO of molecules

	HOMO					LUMO				
	BLYP	B3LYP	B3BP86	BHandHLYP	LC-BLYP[a]	BLYP	B3LYP	B3BP86	BHandHLYP	LC-BLYP[a]
3A	−4.87	−5.83	−6.48	−6.87	−8.58	−2.73	−2.35	−3.00	−1.34	−0.17
4A	−5.76	−6.82	−7.53	−7.95	−9.69	−4.45	−4.15	−4.77	−3.23	−2.10
PEN	−3.88	−4.61	−5.28	−5.31	−6.73	−2.73	−2.40	−3.08	−1.42	−0.58
PF-PEN	−4.52	−5.39	−6.01	−6.29	−7.57	−3.55	−3.37	−4.00	−2.55	−1.70
1 $C_{16}S_8$	−4.78	−5.74	−6.40	−6.77	−8.41	−1.73	−1.07	−1.68	−0.04	1.15

[a] Values calculated using the LC-BLYP/6-31G(d,p) level with the B3LYP/6-31G(d,p) geometries.

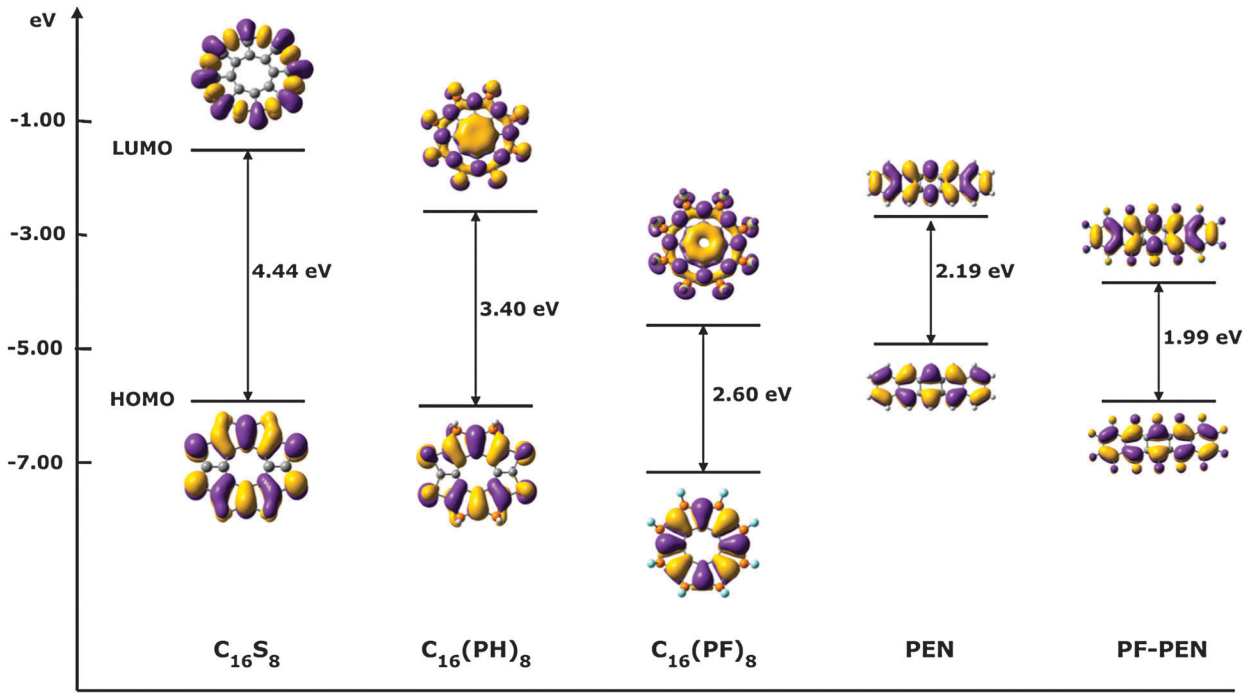

Fig. 4 Shapes of HOMO and LUMO of the molecules considered and their energy levels.

PEN and **PF-PEN** are −5.3 eV and −6.0 eV, respectively, that are comparable to the experimental values of 5.1 eV for **PEN** and of 5.8 eV for **PF-PEN**.[49] However, the B3LYP value of 5.74 eV of $C_{16}S_8$ turns out to be closer to the experimental value of 5.70 eV.[15] For LUMO energies, while the B3P86 value of −3.1 eV for **PEN** agrees well with the experimental value of −3.0 eV, the BHandHLYP LUMO energy of **PF-PEN** is closer to the reality.[49] These differences arise in part from the fact that the experimental results are obtained in solution, whereas our theoretical predictions are for gas phase species. Thus, the relative positions within a series of related molecules considered in this work are more meaningful than their absolute values. At the B3P86/6-31G(d,p) level of theory, the HOMO energy level of **3A** $C_{16}(PH)_8$ is equal to 6.5 eV slightly higher as compared to **1** $C_{16}S_8$ (HOMO = −6.4 eV) and **PEN** (HOMO = −5.3 eV), whereas its LUMO energy level is increased considerably from −1.7 eV for **1** to −3.0 eV for **3A**. The LUMO energy level of **3A** $C_{16}(PH)_8$ is close to the work function of 2.9 eV of the calcium electrode. As expected, substitution of H-atoms of **3A** by F-atoms remarkably decreases both LUMO and HOMO energy levels of the resulting **4A**. Similar to the cases of pentacene and its perfluoropentacene derivative, the LUMO energy level of $C_{16}(PF)_8$ is shifted down more than that of its HOMO (Fig. 4). Accordingly, the LUMO energy level of $C_{16}(PF)_8$ of −4.8 eV could lead to a very low barrier of electron injection of 0.33 eV when the gold electrode is used. These values appear to be much better as compared to those of **PF-PENT** that is a well-known typical n-type semiconductor (Table 2). The ionization energy (IE) and electron affinity (EA) of the compounds considered are calculated from energy difference between the neutral species, cationic species (for IE) and anionic species (for EA). Table 3 shows that the IEs obtained at the B3P86/6-31G(d,p) and B3LYP/6-311++G(d,p) levels are in good agreement with available experimental data. The BHandHLYP also provides good estimates, while BLYP values are somewhat smaller. This can be understood by the fact that the BLYP functional provides less good geometrical parameters. In another view, the HOMO energy levels are considered to be equal to IEs. Table 2 shows that the HOMO of **PEN** and **PF-PEN** of 6.7 and 7.6 eV, respectively, obtained from the LC-BLYP functional are in good agreement with the experimental IE values in the gas phase of 6.54 eV for **PEN**[50] and 7.50 eV for **PF-PEN**.[51] IEs derived from other functionals are

Table 3 Ionization energy (IE) and electron affinity (EA) of compounds obtained by using various functionals in conjugation with the 6-31G(d,p) basis set

	Ionization energy (IE, eV)					Electron affinity (EA, eV)				
	B3LYP[a]	B3LYP	B3P86	BHandH	BLYP	B3LYP[a]	B3LYP	B3P86	BHandH	BLYP
3A	7.10	6.90	7.55	7.28	6.38	1.52	1.30	1.95	0.94	1.31
4A	8.44	7.96	8.59	8.36	7.33	3.64	3.09	3.72	2.81	3.02
PEN	6.13[b]	—	6.57[c]	—	—	1.49[b]	—	—	—	—
PF-PEN	7.12[b]	—	—	—	—	2.78[b]	—	—	—	—
1 $C_{16}S_8$	—	—	7.67[c]	—	—	—	—	—	—	—

[a] Values obtained at B3LYP/6-31++G(d,p)//B3LYP/6-31G(d,p). [b] Values obtained from ref. 8. [c] Values obtained from ref. 17.

simply underestimated. This observation agrees well with previous studies on π-conjugated molecules.[53] High IE and low EA values of **3A** and **4A** are important for their stability in different environments.

In a general view, the HOMO and LUMO levels of **3A** vary in an ideal range of semiconducting materials and thus it is suggested for both n- and p-type semiconductors. The derivative **4A** has a too high HOMO energy and is thus only suitable for an n-type semiconductor.

Density of state (DOS)

We probe further the electronic distribution by examining the density of states (DOS) that can be considered as a simple MO energy spectrum of the molecule, whereas the partial density of states (pDOS) are computed only from certain atomic orbitals (AOs) of interest. The DOS plot shows the composition of the MOs involved. The plots of total density of states of **3A** $C_{16}(PH)_8$ and **4A** $C_{16}(PF)_8$ are displayed in Fig. 5a together with that of **1** $C_{16}S_8$. Replacement of S-atoms of **1** by PH- and PF-groups induces significant shifts for frontier orbital energies. Frontier orbitals of $C_{16}(PF)_8$ containing strongly electron withdrawing F-atoms are remarkably down-shifted as compared to $C_{16}(PH)_8$. These predictions agree well with the results that HOMO and LUMO of $C_{16}(PF)_8$ are much lower as compared to those of $C_{16}(PH)_8$ and $C_{16}S_8$ (Table 2).

The partial density (pDOS) distribution on the p_z component that is important for charge mobility of an organic semiconductor is further analyzed in Fig. 5b–d. While p_z-AOs of both carbon and sulfur have significant contributions to frontier orbitals of $C_{16}S_8$, only p_z-atomic orbitals of carbon are presented in composition of frontier orbitals of $C_{16}(PF)_8$ and $C_{16}(PH_8)$. Additionally, the contributions of carbon and sulfur atoms to the HOMO of $C_{16}S_8$ differ considerably from those to its LUMO. This is probably a reason for why the reorganization energy for the electron of the sulflower is much higher as compared to those of the P-flowers.

Reorganization energies

In order to evaluate electron and hole mobility of a molecule, the reorganization energies need to be considered. The reorganization energies are defined as the sum of geometrical relaxation energies when the species goes from the neutral state geometry to a charged state geometry, and *vice versa*. A description of these terms on a potential energy surface is schematically shown in Fig. 6. Accordingly, a molecule has high charge mobility when it has low reorganization energies. The latter can be defined as follows:

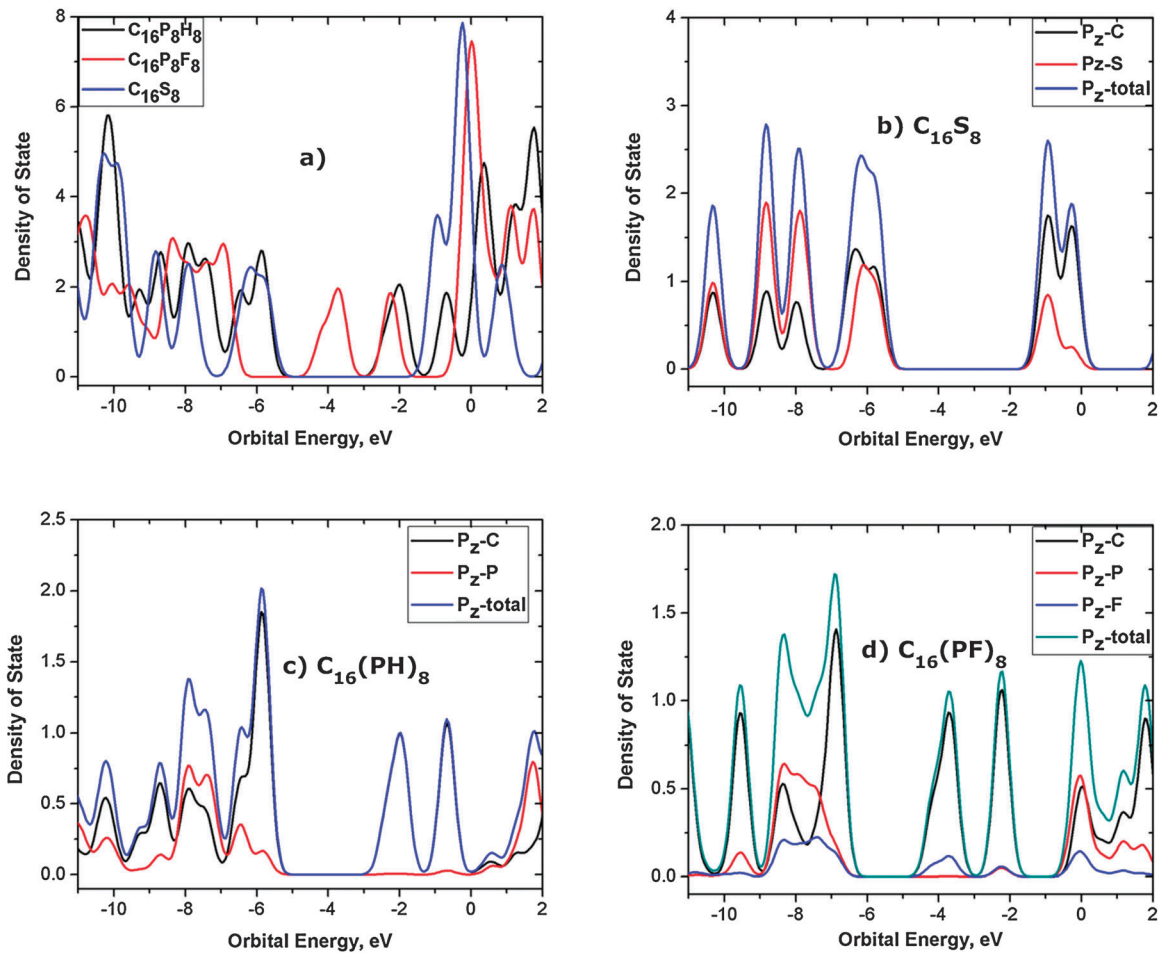

Fig. 5 The plots of (a) total density of state (DOS) of molecules and partial density of state (pDOS) on p_z-distribution of (b) **1** $C_{16}S_8$, (c) **3A** $C_{16}(PH)_8$ and (d) **4A** $C_{16}(PF)_8$.

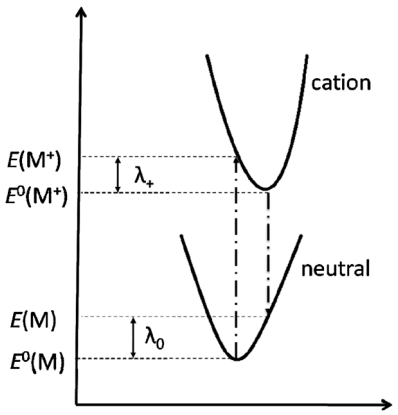

Fig. 6 A schematic plot defining the reorganization energy.

$$\lambda_h = \lambda_0 + \lambda_+ = [E(M) - E^0(M)] + [E(M^+) - E^0(M^+)] \quad (2)$$

$$\lambda_e = \lambda_0 + \lambda_- = [E(M) - E^0(M)] + [E(M^-) - E^0(M^-)] \quad (3)$$

where λ_h and λ_e are reorganization energies for the hole and electron, respectively; $E(M^+)$ and $E(M^-)$ the total energies of the cationic and anionic states with the optimized geometries of the neutral ground state, respectively; $E(M)$ the total energy of the neutral state with the optimized geometries of the cationic species (for eqn (2)) and of the anionic species (for eqn (3)); $E^0(M)$, $E^0(M^+)$ and $E^0(M^-)$ the total energies of the neutral, cationic and anionic ground state species, respectively.

The hole and electron reorganization energies of **1**, **3A** and **4A** obtained using various computational methods are shown in Table 4, together with those computed for well-known materials such as pentacene, perfluoropentacene.

It can be observed that there is a negligible difference between the reorganization energies obtained by two functionals B3LYP and B3P86. The values obtained using the larger basis set (B3LYP/6-31++G(d,p)) are somewhat smaller than the others. At the B3P86/6-31G(d,p) level, the reorganization energies for the hole (λ_h) and electron (λ_e) of **3A** $C_{16}(PH)_8$ are equal to 0.21 and 0.09 eV, respectively. The latter is interestingly much smaller than that of 0.42 eV of **1** $C_{16}S_8$.[17] Even as compared to **PF-PEN** (λ_e = 0.23 eV at B3LYP/6-31++G(d,p)),[8] the value of 0.09 eV of $C_{16}(PH)_8$ is also remarkably lower. As expected, our predictions show that the reorganization energy is increased from 0.09 eV for **3A** $C_{16}(PH)_8$ to 0.22 eV for **4A** $C_{16}(PF)_8$. The latter is comparable to that of 0.23 eV of **PF-PEN** at the same level.[8]

Although previous studies suggested that the B3LYP functional is the best choice for estimating relaxation energies of oligoacenes,[54] and an increase of HF-exchange ends up increasing relaxation energies, such a trend is not emerged in our computed results (Table 4).

Dimer configurations and rate of charge hopping (*K*)

To probe the charge hopping behavior, we perform calculations on the dimers of the molecules considered by using the B3LYP-D functional that contains dispersion energy (-D). These predictions allow us to examine the rate of charge hopping of charge carriers of molecules **1**, **3** and **4**.

The dimers are thus constructed in a translational parallel manner in which the molecules are situated on the top of each other. This configuration was found to have the highest transfer integral (t) among the dimer configurations of **1**.[12,14] All the dimer geometries are optimized at the B3LYP-D/6-31G(d) level of theory and depicted in Fig. 7. There is a negligible difference between the dimer configuration of $C_{16}S_8$ obtained from our theoretical predictions and that obtained from X-ray structure. The intermolecular distance between two monomers $C_{16}S_8$ is predicted to be 3.83 Å and slightly shorter than the experimental value of 3.90 Å.[15] Interestingly, the intermolecular distance of dimer **3A** ($C_{16}P_8H_8$) is increased to 3.93 Å, whereas that of dimer **4A** ($C_{16}P_8F_8$) becomes somewhat shorter and equal to 3.78 Å.

According to the hopping mechanism, the hole and electron carriers can be jumped between two adjacent molecules of the organic crystals. The rate of charge hopping (K) is usually estimated by using the Marcus–Hush equation:[55]

$$K = \frac{t^2}{\hbar}\sqrt{\frac{\pi}{\lambda k_B T}}\exp\left(\pi - \frac{\lambda}{4k_B T}\right) \quad (4)$$

where t is the transfer integrals between two adjacent molecules, λ the reorganization energies, k_B the Boltzmann constant and T the temperature (298 K in our calculations). Accordingly, a high rate of charge hopping K is obtained when the transfer integral (t) between two molecules is high, and the monomers have low reorganization energy (λ).

The transfer integral can be defined by the following expression:[14,56]

$$t = \langle \phi_i^{0,site1} | F | \phi_j^{0,site2} \rangle \quad (5)$$

where $\phi_i^{0,site1}$ and $\phi_j^{0,site2}$ present the HOMOs–LUMOs of molecules 1 and 2, respectively. F is the Fock operator for a dimer with a density matrix from the noninteracting dimer of $F = SC\varepsilon C^{-1}$. S is an intermolecular overlap matrix, C and ε are the molecular orbital coefficients and energies from one step diagonalization without iteration. More detailed description about the theoretical approaches can be found elsewhere.[8,38]

Table 4 Reorganization energies for the hole (λ_h, eV) and electron (λ_e, eV)

	Reorganization energy for hole (λ_h)					Reorganization energy for electron (λ_e)				
	BLYP	B3LYP[a]	B3LYP	B3P86	BHandHLYP	BLYP	B3LYP[a]	B3LYP	B3P86	BHandHLYP
3A	0.271	0.197	0.203	0.206	0.254	0.087	0.092	0.111	0.092	0.105
4A	0.168	0.293	0.296	0.299	0.324	0.207	0.215	0.235	0.216	0.224
1 $C_{16}S_8$	—	—	—	0.125[b]	—	—	—	—	0.420[b]	—
PEN	—	0.095[c]	—	0.077[b]	—	—	0.130[c]	—	—	—
PF-PEN	—	0.226[c]	—	—	—	—	0.229[c]	—	—	—

[a] Values obtained at B3LYP/6-31++G(d,p)//B3LYP/6-31G(d,p). [b] Values obtained from ref. 17. [c] Values obtained from ref. 8.

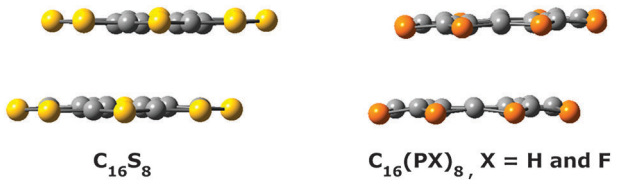

Fig. 7 Dimer configurations of molecules obtained at the B3LYP-D/6-31G(d) level of theory (H- and F-atoms are removed from molecules plotted).

Table 5 Transfer integrals for the electron (t_e, meV) and hole (t_h, meV) and rates of charge hopping K (s^{-1}) of molecules

Molecule	t_e (meV)	t_h (meV)	K_e (s^{-1})	K_h (s^{-1})
3A $C_{16}(PH)_8$	90.3	1.22	2.938×10^{13}	0.013×10^{12}
4A $C_{16}(PF)_8$	99.3	38.1	0.702×10^{13}	0.414×10^{12}
1 $C_{16}S_8$	43.1	24.9		

Accordingly, the transfer integral for the hole (t_h) is equal to the half of energy difference between HOMO and HOMO − 1 of the dimer, while the transfer integral for the electron (t_e) corresponds to the half of energy difference between LUMO and LUMO + 1 of the dimer. Because the failure of the B3LYP functional was shown in evaluating the transfer integral of π-conjugated molecules,[13,33,34,57] the energy levels of these orbitals are obtained by using the PW91/6-31G(d,p) level[58] that was effectively applied to calculate the transfer integrals.[8,14,59] Our calculations interestingly reveal that the transfer integrals for the electron (t_e) of $C_{16}(PH)_8$ and $C_{16}(PF)_8$ are equal to 90.3 meV and 99.3 meV, respectively. These values are very high as compared to that of 43.1 meV of the sulflower **1** obtained using the same computational method. This value was reported to be 54 meV by Mohakud and Pati.[12] The transfer integral for the hole (t_h) of $C_{16}(PH)_8$ is only 1.20 meV that is much lower than those of the $C_{16}S_8$ and $C_{16}(PF)_8$. Consequently, both $C_{16}(PH)_8$ and $C_{16}(PF)_8$ show high rates of charge hopping for the electron, whereas $C_{16}(PH)_8$ exhibits a lower rate of hole hopping (Table 5).

Based on the fundamental characteristics such as low energy barrier for electron injection, low reorganization energy and high rate of electron hopping, we would suggest from our predicted results that both $C_{16}(PH)_8$ **3A** and $C_{16}(PF)_8$ **4A** are excellent candidates for use as an n-type organic semiconductor.

4. Concluding remarks

In this paper, we report on two new P-flower $C_{16}(PH)_8$ and $C_{16}(PF)_8$ molecules that are designed by us on the basis of chemical consideration and subsequently characterized by quantum chemical computations. Our predictions show that both molecules have symmetrical geometries and quasi-planar framework of carbon and phosphorus. The infrared spectra of the new molecules are simulated, and the electron delocalization and aromaticity examined using the electron localization function (ELF).

The electronic structure of both molecules is further investigated by using total and partial density of state (DOS). The fluorinated P-flower $C_{16}(PF)_8$ reveals small energy barrier of electron injection, low reorganization energy and high rate of electron hopping. The parent $C_{16}(PH)_8$ exhibits very low energy barrier of electron injection, remarkably low reorganization energy and high rate of electron hopping. Accordingly, we would suggest that both P-flower molecules are potential candidates for n-type organic semiconductors. It is up to experimental chemists to take up the challenge for their actual synthesis. Let us point out that in a previous study,[60] we theoretically predicted the existence of related phosphole macrocycles, namely the phosphorus-containing porphyrins, which were subsequently prepared in the laboratory.[61]

Acknowledgements

MTN is indebted to the KU Leuven Research Council (GOA, IDO and IUAP programs) and thanks ICST for supporting his stays in Vietnam. TBT thanks the Arenberg Doctoral School for a scholarship.

References

1 C. D. Dimitrakopoulos and P. R. L. Malenfant, *Adv. Mater.*, 2002, **14**, 99, and references therein.
2 H. E. Katz and Z. Bao, *J. Phys. Chem. B*, 2002, **104**, 671.
3 S. F. Nelson, Y. Y. Lin, D. J. Gundlach and T. N. Jackson, *Appl. Phys. Lett.*, 1998, **72**, 1854.
4 C. R. Newman, C. D. Frisbie, D. A. S. Filho, J. L. Bredas, P. C. Ewbank and K. R. Mann, *Chem. Mater.*, 2004, **16**, 4436, and references therein.
5 Y. Inoue, Y. Sakamoto, T. Suzuki, M. Kobayashi, Y. Gao and S. Tokito, *Jpn. J. Appl. Phys.*, 2004, **44**, 3663.
6 N. Koch, A. Wollmer, S. Duhm, Y. Sakamoto and T. Suzuki, *Adv. Mater.*, 2007, **19**, 112.
7 X. K. Chen, L. Y. Zou, J. F. Gou and A. M. Ren, *J. Mater. Chem.*, 2012, **22**, 6471.
8 S. Chai, S. H. Wen, J. D. Huang and K. L. Han, *J. Comput. Chem.*, 2011, 3218.
9 V. C. Sundar, J. Zaumseil, V. Podzorov, E. Menard, R. L. Willett, T. Someya, M. E. Gershenson and J. A. Rogers, *Science*, 2004, **1644**, 303.
10 V. Podzorov, E. Menard, A. Borissov, V. Kiryukhin, J. A. Rogers and M. E. Gershenson, *Phys. Rev. Lett.*, 2004, **93**, 86602.
11 K. Y. Chernichenko, V. V. Sumerin, R. V. Shpanchenko, E. S. Balenkova and G. Nenajdenko, *Angew. Chem., Int. Ed.*, 2006, **45**, 7367.
12 S. Mohakud and S. K. Pati, *J. Mater. Chem.*, 2009, **19**, 4356.
13 G. Gahungu, J. Zhang and T. Barancira, *J. Phys. Chem. A*, 2009, **113**, 255.
14 X. D. Tang, Y. Liao, H. Z. Gao, Y. Geng and Z. M. Su, *J. Mater. Chem.*, 2012, **22**, 6907.
15 A. Dadvand, F. Cicoira, K. Y. Chernichenko, E. S. Balenkova, R. M. Osuma, F. Rosei, V. G. Nenajdenko and D. F. Perepichka, *Chem. Commun.*, 2008, 5354.
16 T. Fujimotor, M. M. Matsushita and K. Awaga, *Appl. Phys. Lett.*, 2010, **97**, 123303.
17 G. Gahungu and J. Zhang, *Phys. Chem. Chem. Phys.*, 2008, **10**, 1743.
18 D. Delaere, A. Dransfeld, M. T. Nguyen and L. G. Vanquickenborne, *J. Org. Chem.*, 2000, **65**, 2631.
19 D. Delaere, M. T. Nguyen and L. G. Vanquickenborne, *Chem. Phys. Lett.*, 2001, **333**, 103.
20 D. Delaere, M. T. Nguyen and L. G. Vanquickenborne, *J. Organomet. Chem.*, 2002, **643**, 194.
21 D. Delaere, M. T. Nguyen and L. G. Vanquickenborne, *Phys. Chem. Chem. Phys.*, 2002, **4**, 1522.
22 D. Delaere, M. T. Nguyen and L. G. Vanquickenborne, *J. Phys. Chem. A*, 2003, **107**, 838.
23 D. Delaere, N. N. Pham-Tran and M. T. Nguyen, *Chem. Phys. Lett.*, 2004, **383**, 138.
24 N. N. Pham-Tran and M. T. Nguyen, *C. R. Chim. Acad. Sci.*, 2010, **13**, 912.

25 M. J. Frisch, et al., *Gaussian 03, Revision C.01*, Gaussian, Inc., Wallingford, CT, 2004.
26 C. Lee, W. Yang and R. G. Parr, *Phys. Rev. B: Condens. Matter*, 1988, **37**, 785.
27 A. D. Becke, *Phys. Rev. A: At. Mol. Opt. Phys.*, 1988, **38**, 3098.
28 A. D. Becke, *J. Chem. Phys.*, 1993, **98**, 5648.
29 J. P. Perdew, *Phys. Rev. B: Condens. Matter*, 1986, **33**, 8822.
30 A. D. Becke, *J. Chem. Phys.*, 1993, **98**, 1372.
31 P. C. Harihara and J. A. Pople, *Theor. Chim. Acta*, 1973, **28**, 213.
32 M. M. Francl, W. J. Petro, W. J. Hehre, J. S. Binkley, M. S. Gordon, D. J. DeFrees and J. A. Pople, *J. Chem. Phys.*, 1982, **77**, 3654.
33 G. Gahungu, B. Zhang and J. P. Zhang, *J. Phys. Chem. C*, 2007, **111**, 4838–4846.
34 D. Jacquemin and E. A. Perpete, *Chem. Phys. Lett.*, 2006, **429**, 147–152.
35 W. J. Hehre, R. Ditchfield and J. A. Pople, *J. Chem. Phys.*, 1972, **56**, 2257.
36 S. Grimme, *J. Comput. Chem.*, 2004, **25**, 1463.
37 S. Grimme, *J. Comput. Chem.*, 2006, **27**, 1787.
38 J. C. Sancho-Garcia, A. J. Perez-Jimenez, Y. Olivier and J. Cornil, *Phys. Chem. Chem. Phys.*, 2010, **12**, 9381.
39 R. Ahlrichs, M. Bär, M. Häser, H. Horn and C. Kölmel, *Chem. Phys. Lett.*, 1989, **162**, 165.
40 M. Kohout, *Dgrid-4.2*, Max-Planck Institut fur Chemische Physik und Fester Stoffe, Dresden, 2007.
41 D. L. Bergman, L. Laaksonen and A. Laaksonen, *J. Mol. Graphics Modell.*, 1997, **15**, 301.
42 A. P. Scott and L. Radom, *J. Phys. Chem. A*, 1996, **100**, 16502.
43 B. Napolion, F. Hagelberg, M. J. Huang, J. D. Watts, T. M. Simeon, D. Vereen, W. L. Walters and Q. L. Williams, *J. Phys. Chem. A*, 2011, **115**, 8682, and references therein.
44 T. Shimanouchi, *Tables of Molecular Vibrational Frequencies Consolidated Volume I*, National Bureau of Standards, 1972, pp. 1–160.
45 A. Becke and K. Edgecombe, *J. Chem. Phys.*, 1990, **92**, 5397.
46 B. Silvi and A. Savin, *Nature*, 1994, **371**, 683.
47 J. C. Santos, W. Tiznado, R. Contreras and P. Fuentealba, *J. Chem. Phys.*, 2004, **120**, 1670.
48 J. C. Santos, J. Andres, A. Aizman and P. Fuentealba, *J. Chem. Theory Comput.*, 2005, **1**, 83.
49 Y. Sakamoto, T. Suzuki, M. Kobayashi, Y. Gao, Y. Fukai, Y. Inoue, F. Sato and S. Tokio, *J. Am. Chem. Soc.*, 2004, **126**, 8138.
50 O. L. Griffith, J. E. Anthony, A. G. Jones and D. L. Lichtenberger, *J. Am. Chem. Soc.*, 2010, **132**, 580.
51 M. C. R. Delgado, K. R. Oiss, D. A. Filho, N. E. Grunn, Y. Sakamoto, T. Suzuki, R. M. Osuna, J. Casado, V. Hernandez, J. T. L. Navarrete, N. G. Martinelli, J. Cornil, R. S. Carrera, V. Coropceanu and J. L. Bredas, *J. Am. Chem. Soc.*, 2009, **131**, 1502.
52 H. Iikura, T. Tsuneda, T. Yanai and K. Hirao, *J. Chem. Phys.*, 2001, **115**, 3540.
53 B. M. Wong and T. H. Hsieh, *J. Chem. Theory Comput.*, 2010, **6**, 3704.
54 R. S. Sanchez-Carrera, V. Coropceanu, D. A. da Silva Filho, R. Friedlein, W. Osikowicz, R. Murdey, C. Suess, W. R. Salaneck and J.-L. Bredas, *J. Phys. Chem. B*, 2006, **110**, 18904.
55 R. A. Marcus, *Rev. Mod. Phys.*, 1993, **65**, 599.
56 X. D. Yang, Q. K. Li and Z. G. Shuai, *Nanotechnology*, 2007, **18**, 424029.
57 A. Datta, S. Mohakud and S. K. Oati, *J. Chem. Phys.*, 2007, **126**, 144710.
58 A. Troisi and G. Orlandi, *Chem. Phys. Lett.*, 2001, **344**, 509.
59 G. Nan and Z. Li, *Org. Electron.*, 2012, **13**, 1229.
60 D. Delaere and M. T. Nguyen, *Chem. Phys. Lett.*, 2003, **376**, 329.
61 Y. Matano, T. Nakabuchi, T. Miyajima, H. Imahori and H. Nakano, *Org. Lett.*, 2006, **8**, 5713.